

# Brown adipose tissue detected by PET/CT imaging is associated with less central obesity

Aileen L. Green<sup>a</sup>, Ulas Bagci<sup>d</sup>, Sarfaraz Hussein<sup>d</sup>, Patrick V. Kelly<sup>c</sup>, Razi Muzaffar<sup>a</sup>, Brent A. Neuschwander-Tetri<sup>b</sup> and Medhat M. Osman<sup>a</sup>

**Purpose** This retrospective review was performed to determine whether patients with brown adipose tissue (BAT) detected by fluorine-18-fluorodeoxyglucose (<sup>18</sup>F-FDG) PET/computed tomography (CT) imaging have less central obesity than BMI-matched control patients without detectable BAT.

**Patients and methods** Thirty-seven adult oncology patients with <sup>18</sup>F-FDG BAT uptake were retrospectively identified from PET/CT studies from 2011 to 2013. The control cohort consisted of 74 adult oncology patients without detectable <sup>18</sup>F-FDG BAT uptake matched for BMI/sex/season. Tissue fat content was estimated by CT density (Hounsfield units) with a subsequent noise removal step. Total fat and abdominal fat were calculated. An automated separation algorithm was utilized to determine the visceral fat and subcutaneous fat at the L4/L5 level. In addition, liver density was obtained from CT images. CT imaging was interpreted blinded to clinical information.

**Results** There was no difference in total fat for the BAT cohort (34 ± 15 l) compared with the controls (34 ± 16 l) ( $P = 0.96$ ). The BAT cohort had lower abdominal fat to total fat ratio compared with the controls (0.28 ± 0.05 vs. 0.31 ± 0.08, respectively;  $P = 0.01$ ). The BAT cohort had a lower visceral fat/(visceral fat + subcutaneous fat) ratio

compared with the controls (0.30 ± 0.10 vs. 0.34 ± 0.12, respectively;  $P = 0.03$ ). Patients with BAT had higher liver density, suggesting less liver fat, compared with the controls (51.3 ± 7.5 vs. 47.1 ± 7.0 HU,  $P = 0.003$ ).

**Conclusion** The findings suggest that active BAT detected by <sup>18</sup>F-FDG PET/CT is associated with less central obesity and liver fat. The presence of foci of BAT may be protective against features of the metabolic syndrome. *Nucl Med Commun* 00:000–000 Copyright © 2017 Wolters Kluwer Health, Inc. All rights reserved.

Nuclear Medicine Communications 2017, 00:000–000

**Keywords:** brown adipose tissue, brown fat, fluorine-18-fluorodeoxyglucose, metabolic syndrome, obesity, PET/CT

<sup>a</sup>Department of Radiology, Division of Nuclear Medicine, Saint Louis University, <sup>b</sup>Department of Internal Medicine, Division of Gastroenterology and Hepatology, Saint Louis University School of Medicine, <sup>c</sup>Department of Statistics, Doisy College of Health Sciences Research Administration, St Louis, Missouri and <sup>d</sup>Department of Electrical and Computer Science, Center for Research in Computer Vision, University of Central Florida, Orlando, Florida, USA

Correspondence to Medhat M. Osman, MD, PhD, Division of Nuclear Medicine & PET/CT, Saint Louis University Hospital, 2nd Floor, 3635 Vista Avenue, St Louis, MO 63110, USA  
Tel: +1 314 577 8047; fax: +1 314 268 5144; e-mail: mosman@slu.edu

Received 10 October 2016 Revised 30 March 2017 Accepted 21 April 2017

## Introduction

Obesity is a global health problem, with more than half a billion adults affected by obesity worldwide [1]. Obesity is associated with increased risks for numerous diseases. Notably, abdominal obesity is a risk factor for the metabolic syndrome [2,3]. When first diagnosed, patients with the metabolic syndrome have twice the risk of developing cardiovascular disease over the next 5–10 years and they have a five-fold increased risk for type 2 diabetes mellitus compared with patients without the syndrome [4–7].

The location of the abdominal fat (AF) is an important risk factor for the metabolic syndrome. Studies indicate that abdominal visceral fat (VF) is more closely associated with the metabolic syndrome than subcutaneous fat (SF) [8,9]. Nonalcoholic fatty liver disease (NAFLD) is associated with an increased risk of metabolic syndrome in increased VF (ref) and most patients with NAFLD have one or more features of metabolic syndrome [10].

Brown adipose tissue (BAT) has been shown to generate body heat in mammals (thermogenesis), and it is considered as a natural defense against hypothermia and is protective against obesity [11–13]. However, its role in fat metabolism is unclear. BAT is a sympathetically innervated organ rich in mitochondria that expresses uncoupling proteins that direct metabolic energy into heat rather than ATP synthesis [14,15]. Recent studies in mice have shown a potentially important role for BAT in fat metabolism [16]. Differences in BAT in mice have been implicated in the risk of developing features of the metabolic syndrome [17].

BAT has high metabolic activity and is detectable by fluorine-18-fluorodeoxyglucose (<sup>18</sup>F-FDG) PET/computed tomography (CT) imaging. <sup>18</sup>F-FDG uptake by BAT has been reported in the cervical, supraclavicular, mediastinal, paraspinous, and perinephric regions of adults [18–20]. The prevalence of <sup>18</sup>F-FDG BAT uptake in patients ranges between 2.5 and 8.5%, with a female and

cold weather predominance, and its presence is associated inversely with age and BMI [18–22].

In this investigation, we tested the hypothesis that patients with BAT detected by  $^{18}\text{F}$ -FDG PET/CT imaging have less central obesity compared with BMI-matched control patients without detectable BAT at the time of  $^{18}\text{F}$ -FDG PET imaging.

## Patients and methods

This study received institutional review board approval for a retrospective study of PET/CT and clinical data. The need for written informed consent was waived.

### Patient selection

We performed a retrospective review of 4458 consecutive  $^{18}\text{F}$ -FDG PET/CT reports of oncologic patients from a single institution between 2011 and 2013 to identify studies with  $^{18}\text{F}$ -FDG uptake by BAT and matched patients for the control cohort. The control cohort consisted of two patients for each patient with BAT for a total of 74 controls patients matched for sex and BMI  $\pm 10\%$ . Furthermore, because BAT is increased by cold temperature exposure, we matched the BAT and control cohorts for the month in which the PET/CT study was carried out (essentially matched for season).

### Inclusion and exclusion criteria

From the 4458 consecutive  $^{18}\text{F}$ -FDG PET/CT reports, there were 46 unique adult patients (age  $\geq 21$  years) whose PET/CT reports specified the presence of BAT. Seven patients with  $^{18}\text{F}$ -FDG avid liver lesions were excluded. After review of the images, one patient was excluded for only negligible PET/CT evidence of BAT reported in the paravertebral region. Another was excluded as  $^{18}\text{F}$ -FDG uptake was associated with interatrial

lipomatous hypertrophy. Therefore, 37 confirmed cases of adult BAT patients without  $^{18}\text{F}$ -FDG avid liver lesions were included in this study. The  $^{18}\text{F}$ -FDG PET/CT scans of control patients were reviewed to confirm the reported absence of BAT.

### PET/CT imaging

An intravenous injection of 5.18 MBq/kg (0.14 mCi/kg)  $^{18}\text{F}$ -FDG was administered to patients with a blood glucose level less than or equal to 200 mg/day after fasting for at least 4 h and in accordance with the standard protocol, all patients were offered a warm blanket to suppress BAT  $^{18}\text{F}$ -FDG uptake and thus improve PET/CT interpretation. Patients sat in a quiet room during the 60 min uptake phase and were instructed to remain quiet and refrain from physical activity. All scans were acquired using a Gemini TF (Philips Medical Systems; Philips, Andover, Massachusetts, USA) PET/CT scanner. The PET component of the PET/CT scanner is composed of lutetium–yttrium oxyorthosilicate-based crystals. Structural information was obtained from the images inferred from 64-slice multidetector helical CT component of the PET/CT scanner without oral or intravenous contrast. CT imaging data were used for anatomy localization by image fusion and the CT transmission map generation. The field of view was from the top-of-head to the bottom-of-feet. The reconstruction process in the scanner was based on the 3D row action maximum likelihood algorithm [23].

### Image analysis

PET/CT images were evaluated retrospectively on the Gemini TF Extended Brilliance Workstation (Philips Medical Systems, Andover, Massachusetts, USA) by a board-certified nuclear medicine physician to confirm the presence or absence of BAT as stated in the PET/CT reports of the patients included in the study. Furthermore, BAT regions were identified by thresholding the PET images with standardized uptake value more than 2, and then applying logical ‘AND’ operation to the fat mask (obtained from CT experiments). A state-of-the-art co-segmentation algorithm was used to determine the boundaries of BAT regions in 3D [24]. Total fat (TF) tissue volume (TF) was determined by a thresholding approach on whole 3D CT images using an interval of  $-190$  to  $-30$  HU. AF was calculated once the abdominal region was separated from the whole-body CT using an anatomical region of interest definition for the abdomen. VF and SF were assessed at the L4/L5 level according to the standard protocol. We have used an automated method for separation of VF and SF, followed by an expert inspection and correction when necessary [25]. Furthermore, liver and spleen density information were recorded as well after appropriate region of interests were placed in the organs that avoided vascular structures. The CT measurements of the average density of the liver and spleen were obtained using regions of interest of 20 and 10 mm diameter, respectively. The density of the spleen in six control cohort patients could not be obtained

**Table 1 Patient characteristics**

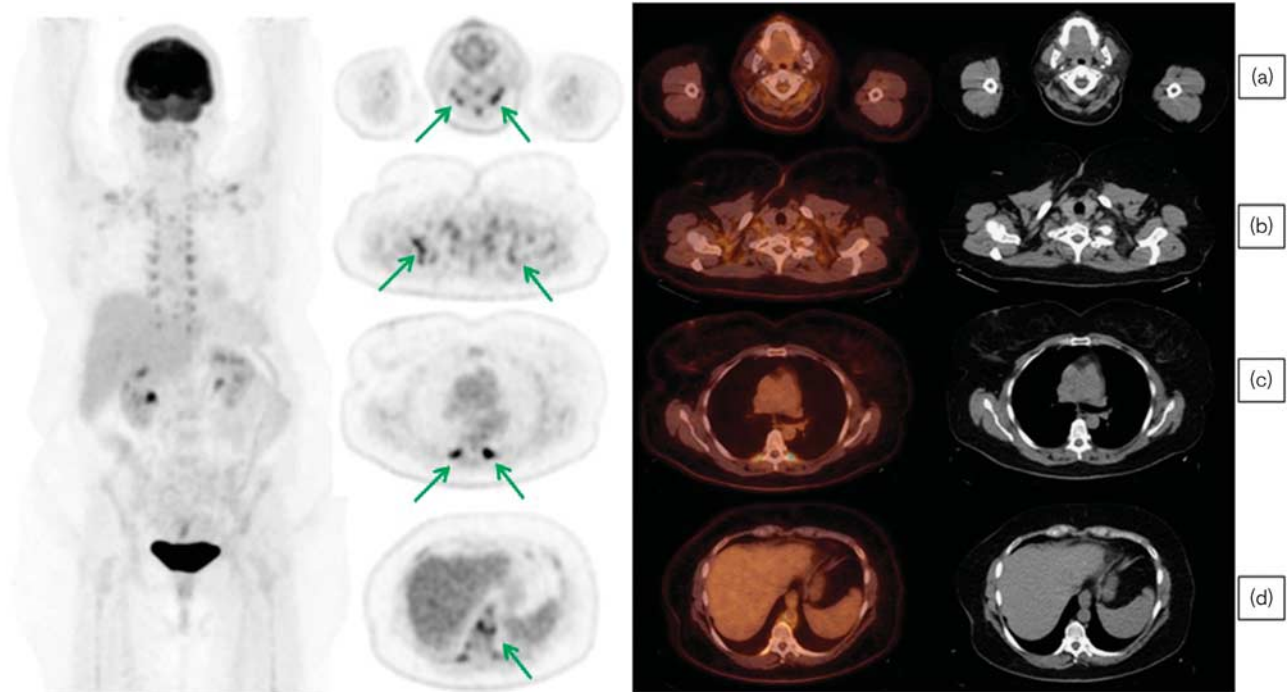
	Brown fat patients	Control patients	<i>P</i> -value
Sex [ <i>n</i> (%)] <sup>a</sup>			
Female	21 (56.8)	42 (56.8)	0.51
Male	16 (43.2)	32 (43.2)	
Age (years) <sup>b</sup>			
Mean $\pm$ SD	50 $\pm$ 16	52 $\pm$ 14	0.17
Median (range)	51 (22–84)	54 (20–83)	
Race [ <i>n</i> (%)] <sup>c</sup>			
White	30 (83)	56 (76)	0.52
Black	6 (17)	18 (24)	
Unknown	1 (NA)	0	
BMI (kg/m <sup>2</sup> ) <sup>b</sup>			
Mean $\pm$ SD	27 $\pm$ 7	27 $\pm$ 6	1.00
Median (range)	26 (18–43)	26 (16–43)	
Weight (kg) <sup>b</sup>			
Mean $\pm$ SD	78 $\pm$ 21	79 $\pm$ 23	0.84
Median (range)	74 (49–130)	74 (45–149)	
Height (m) <sup>b</sup>			
Mean $\pm$ SD	1.7 $\pm$ 0.1	1.7 $\pm$ 0.1	0.80
Median (range)	1.7 (1.5–1.9)	1.7 (1.5–1.9)	

<sup>a</sup>*P*-value determined by a one-sample binomial test.

<sup>b</sup>*P*-value determined by a *t*-test.

<sup>c</sup>*P*-value determined by Pearson's  $\chi^2$ -test.

Fig. 1



Representative brown adipose tissue PET/CT Images. PET/CT images from a 57-year-old obese (BMI = 42.6) White female patient with thymic carcinoma who had a PET/CT study in the summer. The patient was imaged from the top of the skull to the mid-thighs. The first image is a maximal intensity projection PET image. Rows (a–d) show the transaxial PET, fused, and CT images respectively. The images show fluorine-18-fluorodeoxyglucose brown adipose tissue uptake (arrows) in the cervical (row a), supraclavicular (row b), axillary (row b), paraspinous (row c), and para-aortic (row d) regions.

Table 2 Total fat and abdominal fat

	Brown fat patients	Control patients	P-value*
TF (l)	34 ± 15	34 ± 16	0.96
AF (l)	9.9 ± 5.4	11.1 ± 6.5	0.17
AF/TF	0.28 ± 0.05	0.31 ± 0.08	0.01

AF, abdominal fat; TF, total fat.

\*P-value determined by a *t*-test.

Table 3 Visceral fat and subcutaneous fat

	Brown fat patients	Control patients	P-value*
VF (cm <sup>2</sup> )	124 ± 71	145 ± 84	0.09
SF (cm <sup>2</sup> )	299 ± 157	289 ± 161	0.74
VF/(VF + SF)	0.30 ± 0.10	0.34 ± 0.12	0.03

SF, subcutaneous fat; VF, visceral fat.

\*P-value determined by a *t*-test.

because of previous splenectomy. CT imaging was interpreted blinded to clinical information.

### Patient characteristics and data collection

The PET/CT reports were reviewed to identify the sex and age for each patient. The stored data from PET/CT acquisition included the patient's height and weight on the date of the study. BMI was calculated using the

formula  $\text{weight}(\text{kg})/\text{height}^2(\text{m}^2)$ . Race was determined by review of the patient's medical record.

### Statistical methods

The mean differences in age, height, weight, and BMI between the BAT and the control cohort were compared using Student's *t*-test analysis. A Pearson's  $\chi^2$ -test was used to test associations between racial categories and the two cohorts. Sex distribution was examined using a one-sample binomial test. The TF, AF, ratio of AF/TF, VF, SF, ratio of VF/(VF + SF), and liver density of the two cohorts were compared using Student's *t*-test.

## Results

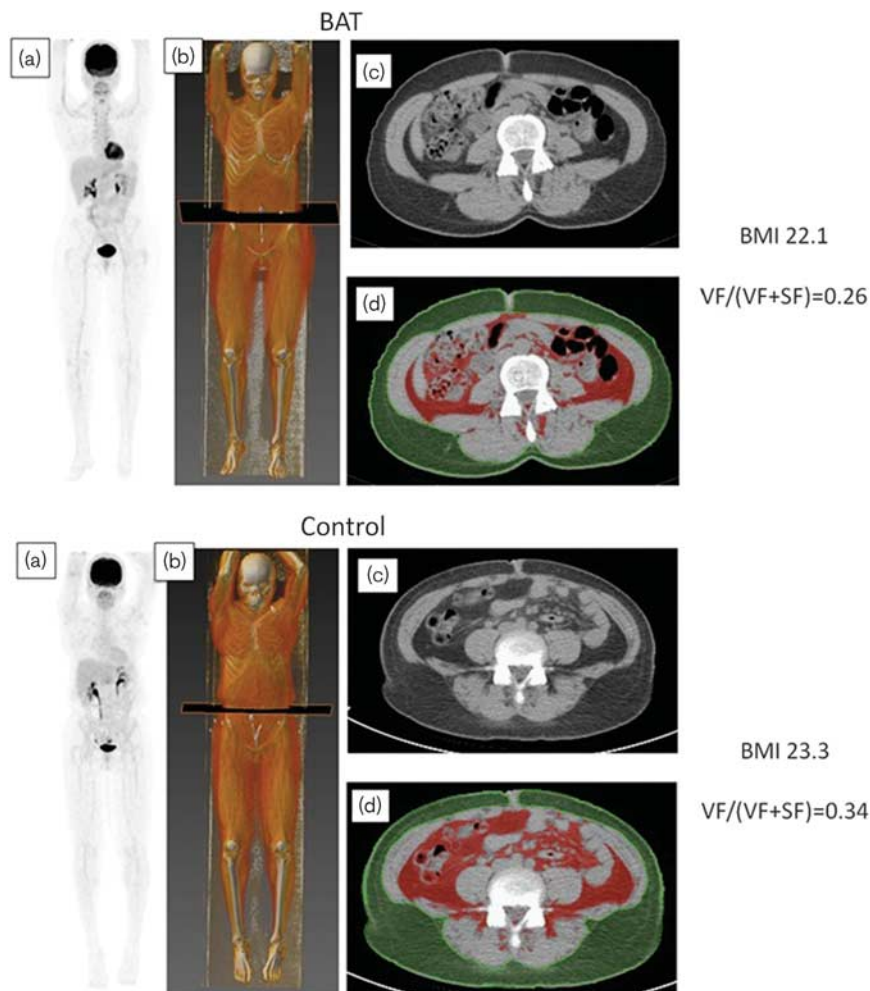
### Patient characteristics

The BAT cohort was mostly White (83.3%), middle aged (49 ± 16 years), and with a mean BMI of 27 ± 7 kg/m<sup>2</sup>. The average age of the control cohort was 54 ± 14 years, not statistically different from the BAT cohort (*P* = 0.17). There was no statistically significant difference between the two cohorts for sex, race, BMI, height, and weight (Table 1).

### Prevalence of brown adipose tissue

Figure 1 shows representative PET/CT images for a BAT patient. The majority of the BAT cohort had at least

Fig. 2



Representative visceral fat (VF) and subcutaneous fat (SF) images of normal BMI brown adipose tissue (BAT) and control patients. Left, a 53-year-old White woman (BMI=22.1) with gastric adenocarcinoma. Right, a 54-year-old Black woman (BMI=23.3) with ductal adenocarcinoma of the pancreas. Both of these PET/CT studies were carried out in the spring. (a) Maximal intensity projection PET image, (b) volume rendering image, (c) transaxial CT image at the umbilicus, and (d) transaxial CT image at the umbilicus with VF (red) and SF (green) highlighted.

two regions of BAT, with the most common region being the supraclavicular region. The prevalence of BAT in patients studied from 2011 to 2013 was ~1%.

#### Total fat and abdominal fat

Table 2 shows a summary of the TF and AF data for the two cohorts. There was no difference in TF for the BAT cohort ( $34 \pm 15$  l) compared with the controls ( $34 \pm 16$  l) ( $P=0.96$ ), which was expected as the BAT cohort and the control cohort were matched for BMI. There was no difference in AF between the BAT cohort ( $9.9 \pm 5.4$  l) and the controls ( $11.1 \pm 6.5$  l) ( $P=0.17$ ). However, the BAT cohort had a significantly lower ratio of AF/TF ( $0.28 \pm 0.05$ ) compared with the controls ( $0.31 \pm 0.08$ ) ( $P=0.01$ ).

#### Visceral fat and subcutaneous fat

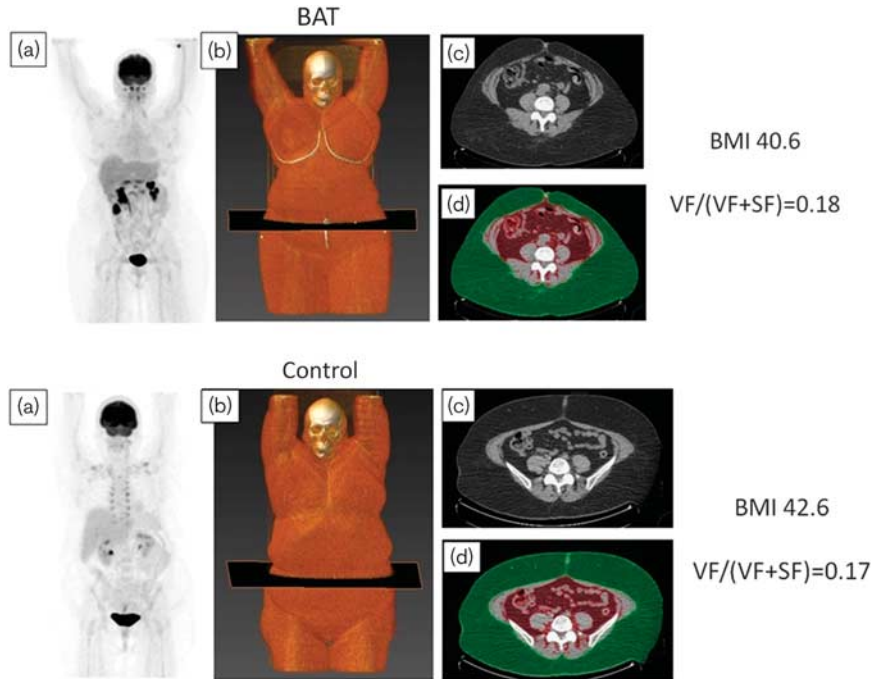
The BAT cohort had a significantly lower ratio of VF/(SF+VF) compared with the controls ( $0.30 \pm 0.10$  vs.

$0.34 \pm 0.12$ , respectively;  $P=0.03$ ). VF in the BAT cohort ( $124 \pm 71$  cm<sup>2</sup>) was not different from the controls ( $145 \pm 84$  cm<sup>2</sup>) ( $P=0.09$ ). There was also no difference in SF for the BAT cohort ( $299 \pm 159$  cm<sup>2</sup>) compared with the controls ( $289 \pm 161$  cm<sup>2</sup>) ( $P=0.74$ ). These results are shown in Table 3 and representative images are shown in Figs 2 and 3.

#### Liver density

The BAT cohort had higher liver density compared with the control cohort ( $51.3 \pm 7.5$  vs.  $47.1 \pm 7.0$  HU) ( $P=0.003$ ). The BAT and control cohorts did not show definite evidence of NAFLD as evidenced by visually decreased liver density on CT and there were no cases where the liver density was less than the spleen density.

Fig. 3



Representative visceral fat (VF) and subcutaneous fat (SF) images of obese BMI brown adipose tissue (BAT) and control patients. Top, a 57-year-old White woman (BMI = 42.6) with thymic carcinoma. Bottom, a 57-year-old Black woman (BMI = 40.6) with adenocarcinoma of the colon. Both of these PET/CT studies were carried out in the summer. (a) Maximal intensity projection PET image, (b) volume rendering image, (c) transaxial CT image at the umbilicus, and (d) transaxial CT image at the umbilicus with VF (red) and SF (green) highlighted.

## Discussion

Studies in mice have shown an inverse correlation between active BAT and obesity. Mice that express markedly less uncoupling protein 1 (UCP1) developed obesity, hyperglycemia, and insulin resistance when subjected to a high-fat diet compared with mice expressing a higher level of UCP1 [16]. Also, the mice with higher levels of UCP1 expression showed significantly more BAT in intermuscular depots [17]. Human studies have shown an inverse relationship between BMI and  $^{18}\text{F}$ -FDG BAT uptake [18,19,22]. This study is unique in that it examined the relationship between BAT and body fat distribution in humans. Our results indicated a significantly lower ratio of AF/TF and VF/(VF + SF) in patients with active BAT as assessed by  $^{18}\text{F}$ -FDG PET/CT studies compared with BMI-matched controls without active BAT. The results are important, given that central obesity is a major risk factor for the metabolic syndrome and its associated comorbidities. Prospective human studies need to be carried out to verify these results and assess for health problems associated with obesity.

The BAT of mice has been shown to oxidatively metabolize fat from triglyceride-rich lipoproteins by thermogenesis during extreme cold exposure [21]. This is different than white adipose tissue, which incorporates

fatty acids from triglyceride-rich lipoproteins into stored triglyceride [26]. Our data showing a higher liver density in the BAT cohort versus controls supports the idea that diversion of fat to oxidative pathways in BAT may reduce the amount of fat in the liver. Although this study did not show overt evidence of NAFLD by CT in either the BAT or the control cohorts, CT imaging is not as sensitive for detecting minor degrees of liver fat [27].

A review by Neuschwander-Tetri [28] challenges the idea that nonalcoholic steatohepatitis, the form of NAFLD at greatest risk for progression to cirrhosis, is caused by triglyceride accumulation in hepatocytes leading to oxidant stress, inflammation, and fibrosis. More important is the source of and fates of fatty acids in the liver, with the best therapies focused on interventions that limit fatty acid exposure in the liver because of increased flux from lipolysis of adipose TG or de-novo lipogenesis in the liver [28].

BAT is one tissue that can oxidatively metabolize fatty acids and thus reduce the flux to the liver. BAT is under adrenergic control and has a predominance of  $\beta_3$ -adrenergic receptors [29].  $\beta_3$ -Agonists are a class of drugs that can potentially stimulate BAT. Cypess *et al.* [30] reported a clinical trial of men treated with high doses of oral mirabegron, a  $\beta_3$ -adrenergic receptor agonist approved for the treatment of overactive bladder,

showing higher BAT metabolic activity and increased resting metabolic rate compared with treatment with placebo [30]. The limitation in using  $\beta_3$ -adrenergic receptor agonists is their lack of selectivity (i.e. stimulation of  $\beta_1$ -adrenergic receptors) and potential adverse cardiovascular effects.

Cold exposure may increase BAT and nonshivering thermogenesis in humans [31,32]. Therefore, cold-induction therapy could be an option to help maintain significant deposits of active BAT into adulthood to treat metabolic diseases.

A limitation of this study is that it was retrospective and we could not acquire quantitative data on nonshivering thermogenesis, energy expenditure, and fasting lipid panels to assess for dyslipidemia. Another limitation is its small sample size. The institutional use of warming blankets may have lowered the prevalence of BAT in our patients compared with previously reported studies. Although the sample size is small, it is larger than other recently published studies of BAT in humans, and included a broader range of patients with respect to age, sex, and BMI. Cancer or cancer therapy may affect adiposity and BAT activity. As both the BAT and the control cohort had cancer and/or cancer therapy, the potential for this to be a confounding influence on BAT activity may be balanced between the two groups. It is possible that some chemotherapy agents can induce or suppress BAT activity and future studies to investigate the effect of chemoradiation therapy on BAT activity may be warranted. Such studies could provide insights into drugs that stimulate or impair BAT activation and help guide therapeutic approaches to the metabolic syndrome.

## Conclusion

We carried out a retrospective analysis of PET/CT studies and clinical data of a BAT cohort and BMI/sex/season-matched control cohort, which did not differ significantly in age, to examine the relationship between BAT and central obesity, an important risk factor for metabolic syndrome. Specifically, we tested the hypothesis that patients with BAT detected by  $^{18}\text{F}$ -FDG PET/CT imaging have less central obesity compared with BMI-matched control patients without BAT. The findings suggest that active BAT detected by  $^{18}\text{F}$ -FDG PET/CT may be associated with less central obesity. Furthermore, the findings indicate that active BAT detected by  $^{18}\text{F}$ -FDG PET/CT may be protective against the accumulation of VF.

## Acknowledgements

The authors thank Holly Karsch, who provided the PET/CT database.

## Conflicts of interest

There are no conflicts of interest.

## References

- 1 World Health Organization World Health Organization. Global status report on noncommunicable diseases. *Chapter 1: Burden, mortality, morbidity and risk factors*. Geneva, Switzerland: World Health Organization; 2010. pp. 35–36.
- 2 Despres JP, Lemieux I. Abdominal obesity and metabolic syndrome. *Nature* 2006; **444**:881–887.
- 3 Alberti KGMM, Zimmet P, Shaw J. Metabolic syndrome – a new world-wide definition. A consensus statement from the international diabetes federation. *Diabet Med* 2006; **23**:469–480.
- 4 Grundy SM, Cleeman JI, Daniels SR, Donato KA, Eckel RH, Franklin BA, et al. American Heart Association: National Heart, Lung and Blood Institute. Diagnosis and management of the metabolic syndrome: an American Heart Association/National Heart, Lung and Blood Institute Scientific statement. *Circulation* 2005; **112**:2735–2752.
- 5 Gami AS, Witt BJ, Howard DE, Erwin PJ, Gami LA, Somers VK, Montori VM. Metabolic syndrome and risk of incident cardiovascular events and death: a systematic review and metaanalysis of longitudinal studies. *J Am Coll Cardiol* 2007; **49**:403–414.
- 6 Grundy SM. Metabolic syndrome pandemic. *Arterioscler Thromb Vasc Biol* 2008; **28**:629–636.
- 7 Nichols GA, Moler EJ. Diabetes incidence for all possible combinations of metabolic syndrome components. *Diabetes Res Clin Pract* 2010; **90**:115–121.
- 8 Shah RV, Murthy VL, Abbasi SA, Blankstein R, Kwong RY, Goldfine AB, et al. Visceral adiposity and the risk of metabolic syndrome across body mass index. *JACC Cardiovasc Imaging* 2014; **7**:1221–1235.
- 9 Fox CS, Massaro JM, Hoffmann U, Pou KM, Maurovich-Horvat P, Liu CY, et al. Abdominal visceral and subcutaneous adipose tissue compartments: association with metabolic risk factors in the Framingham Heart Study. *Circulation* 2007; **116**:39–48.
- 10 Rector RS, Thyfault JP, Wei Y, Ibdah JA. Non-alcoholic fatty liver disease and the metabolic syndrome: an update. *World J Gastroenterol* 2008; **14**:185–192.
- 11 Lee P, Swarbrick MM, Ho KK. Brown adipose tissue in adult humans: a metabolic renaissance. *Endocr Rev* 2013; **34**:413–438.
- 12 Takx RA, Ishai A, Truong QA, MacNabb MH, Scherrer-Crosbie M, Tawakol A. Supraclavicular brown adipose tissue  $^{18}\text{F}$ -FDG uptake and cardiovascular disease. *J Nucl Med* 2016; **57**:1221–1225.
- 13 Chen KY, Cypess AM, Laughlin MR, Haft CR, Hu HH, Bredella MA, et al. Brown Adipose Reporting Criteria in Imaging Studies (BARCIST 1.0): recommendations for standardized FDG-PET/CT experiments in humans. *Cell Metab* 2016; **24**:210–222.
- 14 Enerack S. Human brown adipose tissue. *Cell Metab* 2010; **11**:248–252.
- 15 Cannon B, Nedergaard J. Brown adipose tissue: function and physiological significance. *Physiol Rev* 2004; **84**:277–359.
- 16 Bartelt A, Bruns OT, Reimer R, Hohenberg H, Ilttrich H, Peldschus K, et al. Brown adipose tissue activity controls triglyceride clearance. *Nat Med* 2011; **17**:200–205.
- 17 Almind K, Manieri M, Sivitz WI, Cinti S, Kahn CR. Ectopic brown adipose tissue in muscle provides a mechanism for differences in risk of metabolic syndrome in mice. *Proc Natl Acad Sci USA* 2007; **104**:2366–2371.
- 18 Cypess A, Lehman S, Williams G, Tal I, Rodman D, Goldfine AB, et al. Identification and importance of brown adipose tissue in adult humans. *N Engl J Med* 2009; **360**:1509–1517.
- 19 Cohade C. Altered biodistribution on FDG-PET with emphasis on brown fat and insulin effect. *Semin Nucl Med* 2010; **40**:283–293.
- 20 Cohade C, Osman M, Pannu H, Wahl R. Uptake in supraclavicular area fat ('USA-fat'): description on  $^{18}\text{F}$ -FDG PET/CT. *J Nucl Med* 2003; **44**:170–176.
- 21 Lee P, Greenfield J, Ho K, Fulham M. A critical appraisal of the prevalence and metabolic significance of brown adipose tissue in adult humans. *Am J Physiol Endocrinol Metab* 2010; **299**:E601–E606.
- 22 Cohade C, Mourtzikos KA, Wahl RL. 'USA-fat' – prevalence is related to ambient outdoor temperature – evaluation with  $^{18}\text{F}$ -FDG PET/CT. *J Nucl Med* 2003; **44**:1267–1270.
- 23 Dorfman RE, Alpern MB, Gross BH, Sandler MA. Upper abdominal lymph nodes: criteria for normal size determined with CT. *Radiology* 1991; **180**:319–322.
- 24 Bagci U, Udupa JK, Mendhiratta N, Foster B, Xu Z, Yao J, et al. Joint segmentation of anatomical and functional images: applications in quantification

- of lesions from PET, PET/CT, MRI-PET, and MRI-PET-CT images. *Med Image Anal* 2013; **17**:929–945.
- 25 Tong Y, Udupa JK, Toriqian DA. Optimization of abdominal fat quantification on CT imaging through use of standard anatomic space: a novel approach. *Med Phys* 2014; **41**:063501.
- 26 Williams KJ, Fisher EA. Globular warming: how fat gets to the furnace. *Nat Med* 2011; **17**:157–159.
- 27 Saadeh S, Younossi ZM, Remer EM, Gramlich T, Ong JP, Hurley M, *et al.* The utility of radiological imaging in nonalcoholic fatty liver disease. *Gastroenterology* 2002; **123**:745–750.
- 28 Neuschwander-Tetri BA. Hepatic lipotoxicity and the pathogenesis of nonalcoholic steatohepatitis: the central role of nontriglyceride fatty acid metabolites. *Hepatology* 2010; **52**:774–788.
- 29 Collins S, Cao W, Robidoux J. Learning new tricks from old dogs: beta-adrenergic receptors teach new lessons on firing up adipose tissue metabolic. *Mol Endocrinol* 2004; **18**:2123–2131.
- 30 Cypess AM, Weiner LS, Roberts-Toler C, Franquet Elia E, Kessler SH, Kahn PA, *et al.* Activation of human brown adipose tissue by a beta 3 adrenergic receptor agonist. *Cell Metab* 2015; **21**:33–38..
- 31 Van der Lans A, Hoeks J, Brans B, Vijgen GH, Visser MG, Vosselman MJ, *et al.* Cold acclimation recruits human brown fat and increases nonshivering thermogenesis. *J Clin Invest* 2013; **123**:3395–3403..
- 32 Yoneshiro T, Aita S, Matsushita M, Kayahara T, Kameya T, Kawai Y, *et al.* Recruited brown adipose tissue as an antiobesity agent in humans. *J Clin Invest* 2013; **123**:3404–3408.